International Journal of Automotive Technology, Vol. 19, No. 6, pp. 1081–1089 (2018)
DOI 10.1007/s12239–018–0106–0

Copyright © 2018 KSAE/ 105–16
pISSN 1229–9138/ eISSN 1976–3832

OPTIMIZATION OF GEAR RATIO OF IN-WHEEL MOTOR VEHICLE CONSIDERING PROBABILISTIC DRIVER MODEL

Kihan Kwon, Minsik Seo and Seungjae Min*

Department of Automotive Engineering, Hanyang University, Seoul 04763, Korea

(Received 16 August 2017; Revised 25 March 2018; Accepted 30 May 2018)

ABSTRACT–A reduction gear of an in-wheel motor vehicle is mounted between a traction motor and wheel, to increase the wheel torque and decrease the rotational speed. To improve the energy efficiency of a vehicle, the determination of the optimal gear ratio is an important factor in the design of the reduction gear. This paper presents an optimization procedure to obtain the optimal gear ratio of an in-wheel motor vehicle that minimizes the electric energy consumption. Using a model-based design, a dynamic simulation model of a vehicle was developed for an analysis of the energy efficiency. Owing to a variation in energy efficiency across drivers, a probabilistic driver model that includes driver characteristics is employed. To reduce excessive calculations, a surrogate model was constructed for the optimization. The optimal gear ratio for saving energy was obtained, and the usefulness of the proposed optimization procedure was shown through a comparison of the results of the optimal gear ratio and the energy efficiency achieved between deterministic and probabilistic approaches.

KEY WORDS : In-wheel motor vehicle, Gear ratio, Energy efficiency, Probabilistic driver model, Surrogate model

NOMENCLATURE

J_{eq} : equivalent inertia of vehicle at wheel, kgm^2
ω_{whl} : rotational speed of wheel, rad/s
T_{mot} : motor torque, Nm
T_{res} : resistance torque, Nm
r : gear ratio
m_{body} : mass of body, kg
J_{whl} : inertia of wheels, kgm^2
J_{mot} : inertia of motors, kgm^2
R_{tire} : radius of tire, m
V_{veh} : velocity of vehicle, m/s
μ_r : coefficient of rolling resistance
g : gravity acceleration, m/s^2
C_d : coefficient of air resistance
A_{fr} : frontal area, m^2
ρ_{air} : air density, kg/m^3
T_{max} : maximum motor torque, Nm
ω_{mot} : motor speed, rad/s
T_{regen} : maximum regenerative braking torque, Nm
C_{brk} : capacity of braking torque, Nm
V_{bat} : terminal voltage of battery, V
V_{OCV} : open circuit voltage, V
R_{in} : internal resistance, ohm
I_{bat} : load current, A
SOC_{ini} : initial SOC, %
C_{nom} : nominal capacity of battery, As
η : motor efficiency
K : proportional gain
τ_r : reaction time delay, s
τ_n : neuromuscular lag, s

*Corresponding author. e-mail: seungjae@hanyang.ac.kr

1. INTRODUCTION

In the automotive industry, the trend toward electrification has been recognized as a way to solve environmental issues (Lixin, 2009). Hence, many original equipment manufacturers (OEMs) have developed a market for both hybrid electric vehicles (HEVs), which combine an internal combustion engine with an electric motor, and fully electric vehicles (EVs). Using only electric power, EVs, in particular, have no emissions, and are therefore a possible solution to environmental issues (Pi *et al*., 2016). The propulsion system in an EV can be divided into two types. One is a traction motor installed in the center of the chassis, which transfers power to the wheels through the drivetrain, and is used in conventional EVs. The other uses a number of traction motors placed on each wheel, where each motor transfers power to the wheel directly (Kim *et al*., 2013; Wang *et al*., 2014). In this way, more compact and lightweight powertrain systems can be designed. In addition, there are a number of advantages with respect to the mobility control (Kim *et al*., 2010; Ko *et al*., 2016). Thus, in-wheel motor vehicles are taking up a major portion of the EV market.

Reduction gears are installed in the traction motor of each wheel to increase the torque and decrease the rotational speed of the wheel, because a traction motor can

www.manaraa.com

operate at lower torque and a higher speed compared with the required specifications of the vehicle. The gear ratio of the reduction gear has an influence on the energy saving and driving performance, and thus the selection of the optimal gear ratio is an important factor in the vehicle design. In terms of the energy saving, a change in the operating point of the motor, which is determined by the motor toque and speed, has an influence on the motor efficiency. As shown in Figure 1, the torque is increased and the speed is decreased when the gear ratio is decreased under certain driving conditions. In contrast, the torque is decreased and the speed is increased when the gear ratio is increased. Therefore, it is possible to change the operating point for a high efficiency region by selecting the proper gear ratio. In addition, when the operating point at a specific time is changed into a more efficient point by changing to a certain gear ratio, the operating point at another time may be changed into a more inefficient point. Thus, for the selection of the gear ratio, an integrated analysis of the entire driving range should be employed.

Several previous studies have been conducted on improving the energy efficiency in EVs by increasing the number of gears or optimizing the gear ratio. A method that improves the energy efficiency through the use of a continuously variable transmission (CVT) and multiple speed transmissions for changing the motor operation points to a higher efficiency region was developed (Ren *et al*., 2009). However, this approach does not consider optimizing the gear ratios despite the fact that doing so would result in additional energy efficiency. Other studies have optimized the gear ratios over two-speed (Gao *et al*., 2015; Sorniotti *et al*., 2011; Zhou *et al*., 2013) and three-speed (Di Nicola *et al*., 2012) transmissions to improve the driving performance and efficiency of a conventional EV. However, these approaches do not consider the driver characteristics on the gear ratio optimization despite the fact that actual driver behaviors have an influence on the variation in energy efficiency (De Vlieger, 1997; McGordon *et al*., 2011; Son *et al*., 2016).

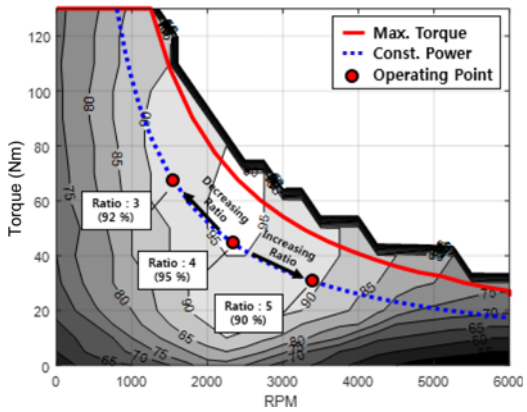

Figure 1. Motor efficiency map: Influence by changing gear ratio.

In this paper, a gear ratio optimization that considers the driver characteristics to improve the energy efficiency of an in-wheel motor vehicle is described. In particular, this paper focuses on the optimization of a single gear ratio, because it is difficult to install a multiple-speed transmission in an in-wheel motor vehicle owing to a limited space and the stability of the gear shift control. To analyze the energy efficiency of a vehicle, a dynamic simulation model was developed using a model-based design. A probabilistic driver model is employed to consider the variation in energy efficiency. Optimization is achieved using a surrogate model to reduce the computational requirements. A design example of a lightweight EV with two in-wheel motors is provided to confirm the usefulness of the proposed procedure, and the gear ratio is optimized for improving the energy efficiency.

2. ANALYSIS MODEL FOR IN-WHEEL MOTOR VEHICLE

A model-based design methodology has numerous advantages when developing a vehicle model. This approach can manage a multidomain system in a single environment, easily handle iterative modeling, and construct a sophisticated design (Mahapatra *et al*., 2008). Using this methodology, a model for an in-wheel motor vehicle is composed of a vehicle powertrain, resistance torque, regenerative braking, battery, and driver models developed through the use of MATLAB/Simulink, the layout of which is illustrated in Figure 2. In particular, the powertrain model is constructed using MapleSim and converted into an S-function for simulation within the MATLAB/Simulink environment.

2.1. Powertrain Model

A powertrain system consists of an in-wheel motor, reduction gear, and wheel. The motor receives torque requested by the driver. The motor power is transmitted to the wheel through the reduction gear. The velocity of the vehicle (V_{veh}) is determined based on the wheel speed (ω_{whl}), through the following equations:

$$J_{\text{eq}}\dot{\omega}_{\text{whl}} = T_{\text{mot}} r - T_{\text{res}}\,, \tag{1}$$

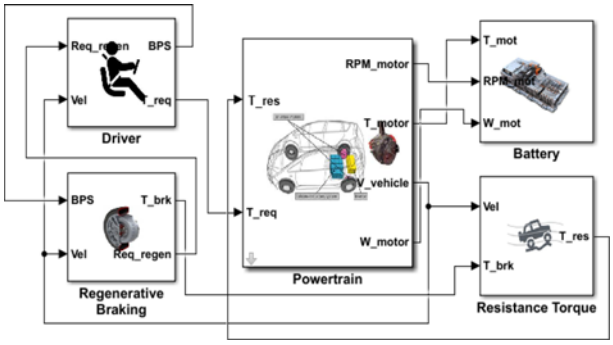

Figure 2. Simulation model.

www.manaraa.com

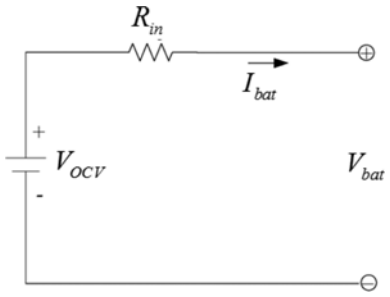

Figure 3. Circuit diagram of the Rint model.

$$J_{\text{eq}} = m_{\text{body}} R_{\text{tire}}^2 + J_{\text{whl}} + J_{\text{mot}} r^2 , \tag{2}$$

$$V_{\text{veh}} = R_{\text{tire}} \omega_{\text{whl}} = R_{\text{tire}} \int \frac{T_{\text{mot}} r - T_{\text{res}}}{J_{\text{eq}}} dt . \tag{3}$$

2.2. Resistance Torque Model

The resistance torque at the wheels can be classified into three components: rolling, aerodynamics, and braking resistance. The total resistance (T_{res}) is estimated based on the velocity of the vehicle (V_{veh}) and the braking torque (T_{brk}), using the following equation (Wang *et al*., 2015):

$$T_{\text{res}} = (\mu_{\text{r}} m_{\text{body}} g + 0.5 C_{\text{d}} A_{\text{fr}} \rho_{\text{air}} V_{\text{veh}}^2) R_{\text{tire}} + T_{\text{brk}} . \tag{4}$$

In this research, the climbing resistance is not considered because the energy efficiency is estimated for driving conditions without a slope.

2.3. Regenerative Braking Model

The battery can be charged by the kinetic energy of the wheels, which is converted by the electric motor during regenerative braking. However, the amount of regenerative braking power is limited based on the various requirements of the regenerative braking system, such as the stability, comfort, and safety (Reif, 2014). Therefore, if such requirements are taken completely into consideration, the control model of the system will become quite complicated. However, a model that applies only the maximum torque capacity of regenerative braking can be used because the effects of the other requirements are insignificant for an analysis of the energy efficiency. For this reason, the regenerative braking model, including the torque distribution between the motor and brake, is simply defined through the following equations:

$$T_{\text{mot}} = \begin{cases} DC \cdot T_{\max}(\omega_{\text{mot}}) & \text{if } DC \geq 0 \\ \dfrac{\max(DC \cdot C_{\text{brk}}, -T_{\text{regen}})}{r} & \text{if } DC < 0 \end{cases} , \tag{5}$$

$$T_{\text{brk}} = \begin{cases} 0 & \text{if } DC \geq 0 \\ DC \cdot C_{\text{brk}} - \max(DC \cdot C_{\text{brk}}, -T_{\text{regen}}) & \text{if } DC < 0 \end{cases} , \tag{6}$$

where DC is the driver's command, the range of which is from −1 to 1. The positive and negative values of DC imply that the vehicle is driving and braking, respectively.

2.4. Battery Model

The energy efficiency can be evaluated based on the difference between the initial and final state of charge (SOC) of the battery. To calculate the SOC consumption after driving, various battery equivalent circuit models, including the Rint, RC, Thevenin, and PNGV models are now widely used (He *et al*., 2011). In this paper, the Rint model, as shown in Figure 3, is applied to analyze the SOC consumption because an analysis of energy efficiency does not need to consider the transient effect when using a capacitor model. The battery model is constructed through the following equations:

$$V_{\text{bat}} = V_{\text{OCV}} - R_{\text{in}} I_{\text{bat}} , \tag{7}$$

$$\Delta SOC = SOC_{\text{ini}} - \frac{100}{C_{\text{nom}}} \int_t I_{\text{bat}}\, dt \ \ [\%] . \tag{8}$$

Based on the relationship between the electric the mechanical energy of the battery during the charging and discharging, I_{bat} is defined through the following equation:

$$I_{\text{bat}} = \begin{cases} \dfrac{T_{\text{mot}} \omega_{\text{mot}}}{\eta(T_{\text{mot}}, \omega_{\text{mot}}) V_{\text{bat}}} & \text{if } T_{\text{mot}} \geq 0 \text{ (discharging)} \\ \dfrac{\eta(T_{\text{mot}}, \omega_{\text{mot}}) T_{\text{mot}} \omega_{\text{mot}}}{V_{\text{bat}}} & \text{if } T_{\text{mot}} < 0 \text{ (charging)} \end{cases} \tag{9}$$

2.5. Driver Model

In this study, a driver transfer function (H) consisting of three parameters (K, τ_{r}, τ_{n}) for the human operator is used through the equation below (Day and Metz, 2000; Noh *et al*., 2014):

$$H(j\omega) = \frac{K e^{-\tau_{\text{r}} j\omega}}{1 + \tau_{\text{n}} j\omega} . \tag{10}$$

The parameters of this function can approximate the degree of aggressive driving, perception of the driver, and the muscle inherent viscosity and inertia. Therefore, the characteristics of the driver can be represented using the parameters K, τ_{r} and τ_{n}. Using the velocity error between the target and vehicle, the model calculates the driver command (DC) determined through Equations (5) and (6), respectively. A block diagram of the driver control system is illustrated in Figure 4.

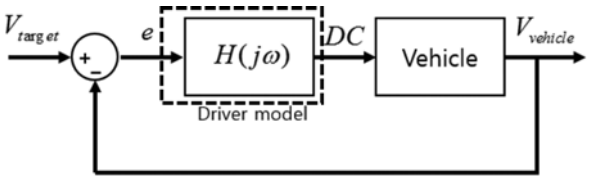

Figure 4. Block diagram of control system.

www.manaraa.com

3. PROBABILISTIC DRIVER MODEL

A variation in driver behavior causes a variation in SOC consumption under the same driving conditions, because the operating point of the motor and the amount of dissipation in the braking energy differ among different driver behaviors. Figures 5 and 6 show the effect on the vehicle velocity, braking torque, and operating point of the motor, based on the level of driver aggression and perception, respectively. As shown in Figure 5, when a driver tends to drive with high aggression, which means the value of K is large, an error between the vehicle velocity and the target velocity is smaller than in the case of low aggression. Because the slope of the velocity during a period of high aggression (θ_h) is higher than that during a period low aggression (θ_l), high aggression can reduce the error faster than low aggression. However, the energy efficiency under high aggression can be worse than under low aggression owing to an increase in the frequency of braking events and the variation in the operating point of the motor. On the other hand, as shown in Figure 6, when a driver has faster perception, which means the value of τ_r is

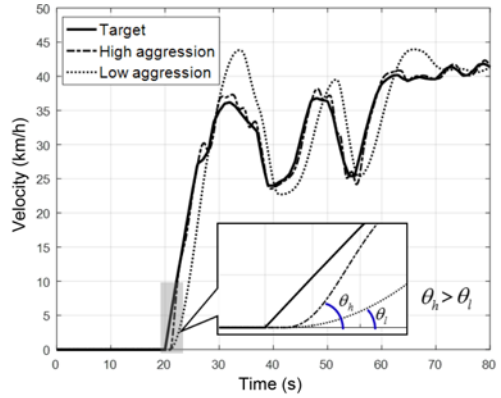

(a) Vehicle velocity

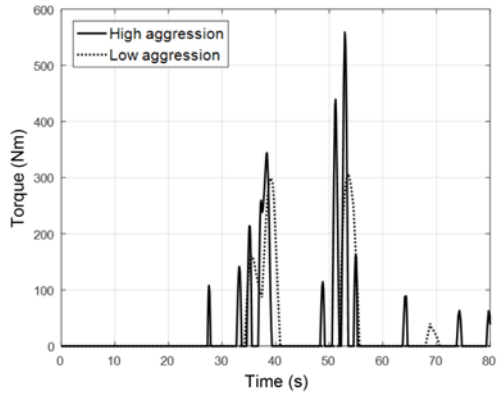

(b) Braking torque

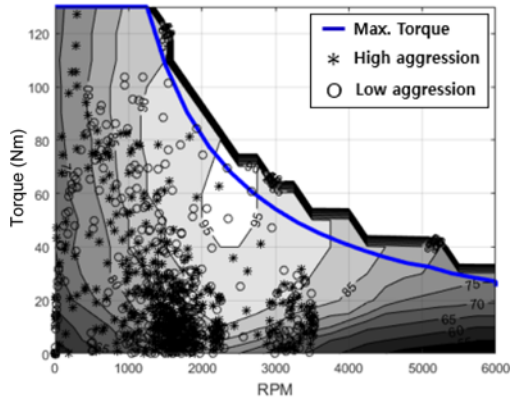

(c) Operating point of motor

Figure 5. Effect of driver aggression.

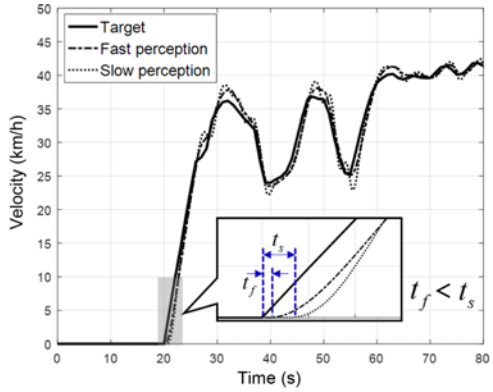

(a) Vehicle velocity

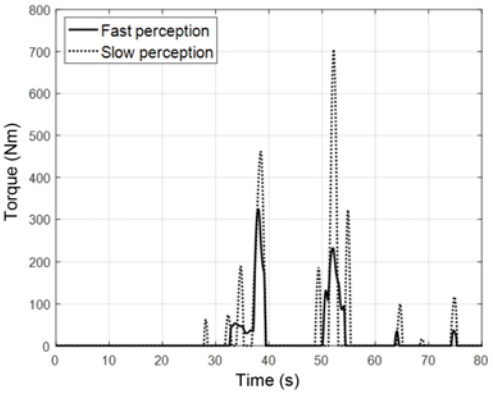

(b) Braking torque

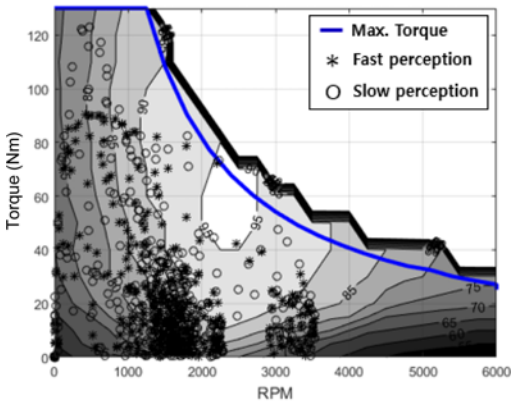

(c) Operating point of motor

Figure 6. Effects of driver perception.

www.manaraa.com

small, the error in the velocity is smaller than that when the driver has slower perception. Because the reaction time for faster perception (t_f) is shorter than for slower perception (t_s), a faster perception can reduce the error more quickly than a slower perception. Such different driver behaviors therefore cause a variation in energy efficiency.

The variation in energy efficiency among drivers can be realized by changing the parameter values (K, τ_r, τ_n) of the driver model. In addition, these parameters can be represented through certain probability density functions based on the driver characteristics. However, it is difficult to define the probability density functions of the parameter values corresponding to the characteristics of the real drivers. In the driver model, as shown in Equation (10), the parameter values are empirically suggested to be $\tau_r > 0.15$ and $0.1 < \tau_n < 0.2$, respectively. The value of parameter K should be as large as possible for control stability and response, because it can be used as a feedback control gain to reduce the error in velocity (Day and Metz, 2000). However, this value should be properly estimated because it is directly related with the driver aggression. For this reason, a definition of the probability density functions requires the experiment result to appropriately represent the driver characteristics.

According to real-world test data among 117 drivers, obtained by the University of Michigan Transportation Research Institute, the variation in fuel efficiency is substantial (LeBlanc *et al*., 2010). In this study, based on this research result, the probability density functions of the parameters are assumed to approximate the test data as closely as possible. Because this result is expressed in terms of fuel consumption, and because the simulation conditions, including the road profile and vehicle specifications, do not match the test conditions, this paper focuses on a tendency in the variation of the SOC consumption based on the effects of the driver.

Figure 7 shows the test data regarding the fuel consumption by individual drivers. Because the range of τ_n is empirically suggested, the function of τ_n is defined through a normal distribution with the mean and standard deviation (0.15, 0.015). However, information regarding

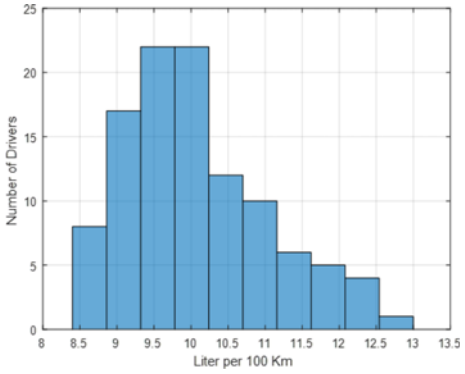

Figure 7. Fuel consumption by individual drivers.

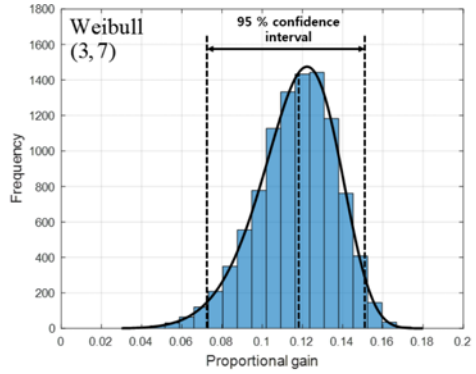

(a) Proportional gain (K)

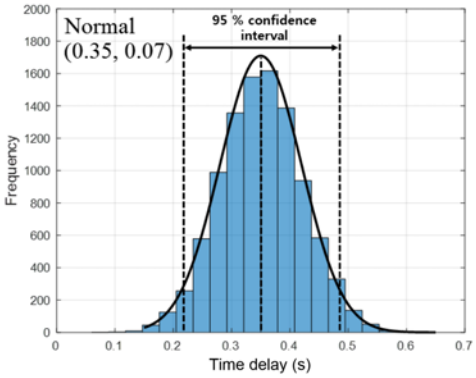

(b) Reaction time delay (τ_r)

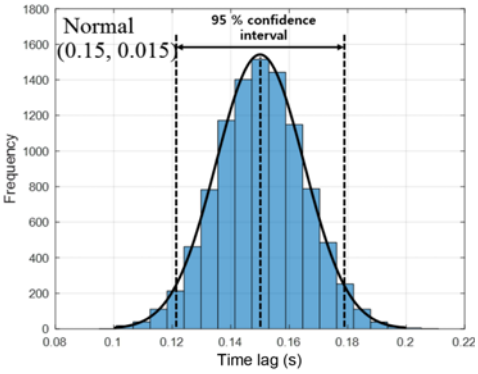

(c) Neuromuscular lag (τ_n)

Figure 8. Probability density functions of parameters in driver model.

the value of K is not suggested, and τ_r is only suggested to be the minimum value.

For this reason, to approximate the tendency of the test data, the function of K is defined based on a Weibull distribution, using the scale and shape parameters (3, 7), and the function of τ_r is defined based on a normal distribution using the mean and standard deviation (0.35, 0.07). The shapes of the probability density functions are shown in Figure 8, and a histogram of the distribution with respect to the SOC consumption through the joint probability density function combined with the three probability density functions (K, τ_r, τ_n) is illustrated in

www.manaraa.com

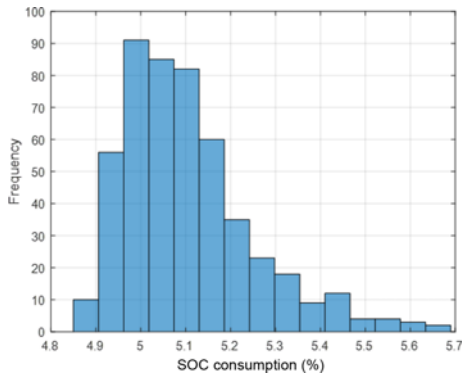

Figure 9. Variation of SOC consumption based on joint probability density function.

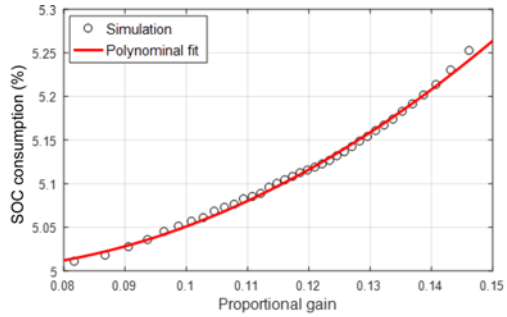

(a) Proportional gain (K): τ_r and τ_n are mean values

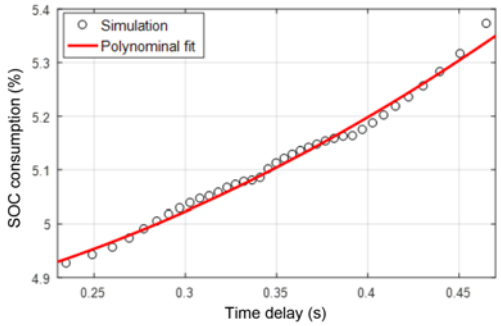

(b) Reaction Time delay (τ_r): K and τ_n are mean values

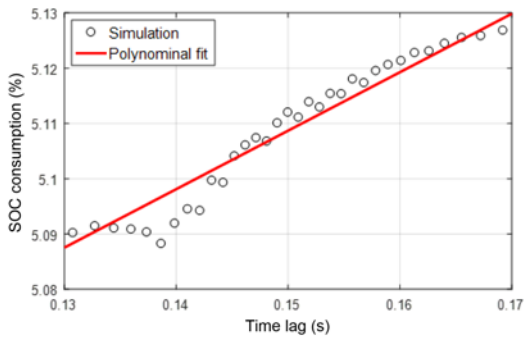

(c) Neuromuscular lag (τ_n): K and τ_r are mean values

Figure 10. Effects of each parameter on SOC consumption.

Figure 9.

Figure 10 shows the simulation results based on the effect of each parameter with respect to the SOC consumption after driving. It should be noted that the energy efficiency is improved when the parameter values are small. This means that the driver behavior shows low aggression, fast perception, and fast muscle reactions. In addition, it can be seen that the effect of τ_n on the SOC consumption is much smaller than that of K and τ_r.

4. GEAR RATIO OPTIMIZATION

A design example of a lightweight EV with two in-wheel motors is applied to the optimization of the gear ratio. The main specifications of the vehicle are summarized in Table 1. To evaluate the energy efficiency, vehicle development organizations have offered the various driving cycles. When the gear ratio optimization is performed for a certain driving cycle, the result may not be acceptable to other cycles. Therefore, the optimization based on the analysis of integrating various cycles can be more appropriate than a certain driving cycle for the robustness of the result. In this reason, three driving cycles are considered which are Urban Dynamometer Driving Schedule cycle (UDDS), Urban Driving Cycle (UDC), and Japan for emission certification and fuel economy for light duty vehicles (JC08). From the SOC consumption results of each cycle, the integrated SOC consumption (ΔSOC_{int}) is defined through the following equation:

$$\Delta SOC_{\text{int}} = \sum_{\text{i=1}}^{3} \frac{\Delta SOC_{\text{i}} \cdot d_{\text{i}}}{d_{\text{sum}}} \tag{11}$$

where i implies the index number with respect to each cycle, d_{i} is the driving distance of each cycle, and d_{sum} is the sum of driving distance over all driving cycles.

Table 1. Vehicle specifications.

	Specifications
Mass of vehicle	1306 kg
Motor	130 Nm / 162 kW / 6000 RPM
Battery	76 Ah / 350 V
Gear ratio	4 : 1
Tire radius	0.275 m

Table 2. Feasible gear ratio conditions.

Constraint	Gear ratio
Maximum speed $\geq$ 110 km/h	$r \leq 5.663$
0 ~ 100 km/h acceleration time $\leq$ 20 s	$r \geq 3.729$

www.manaraa.com

4.1. Problem Formulation

The gear ratio should be determined to satisfy the vehicle dynamic constraints, which are the maximum vehicle speed and the acceleration performance (Gao *et al*., 2015). According to the vehicle simulation, the range of gear ratio that ensures these constraints is shown in Table 2. In conjunction with this range of gear ratio, an objective function that minimizes the integrated SOC consumption over the driving cycles can be formulated as follows:

$$\begin{aligned} &\underset{r}{\text{minimize}} \\ &F = \begin{cases} \Delta SOC_{\text{int}}(r) & \text{(deterministic)} \\ \int_{\Omega} \Delta SOC_{\text{int}}(K,\tau_{\text{r}},\tau_{\text{n}},r)\cdot \Pr(K,\tau_{\text{r}},\tau_{\text{n}})\,d\Omega & \text{(probabilistic)} \end{cases} \\ &\text{subject to } 3.729 \le r \le 5.663, \\ &\text{where } \int_{\Omega} d\Omega = \int_{\text{K}}\int_{\tau_{\text{r}}}\int_{\tau_{\text{n}}} dK d\tau_{\text{r}} d\tau_{\text{n}}, \end{aligned} \tag{12}$$

where Pr represents the probability based on the function of the driver's parameters, and Ω is the probabilistic domain of each parameter.

4.2. Surrogate Model

To increase the accuracy of the integration, 50 sample points of each parameter in the driver model are selected. Because the calculation requires a large number of simulations, using a surrogate model of the integrated SOC consumption (ΔSOC_{int}) with respect to each parameter (K, τ_{r}, τ_{n}, r) is essential to reduce the computational requirements.

Various surrogate models, including rational functions, Kriging models, artificial neural networks (ANNs), splines, and support vector machines (SVMs) have been used to deal with engineering systems that need to invest a lot of computational time to predict the relationship between the system inputs and outputs (Gorissen *et al*., 2010). Because an ANN consists of a combination of nonlinear functions, it is suitable for solving a complex nonlinear system. For this reason, ANNs have been widely used in diverse fields (Changyu *et al*., 2007; Kannan *et al*., 2013; Lerspalungsanti *et al*., 2015).

In this study, 300 sample points from Latin hypercube sampling with respect to four parameters (K, τ_{r}, τ_{n}, r) were selected to construct the surrogate model (ΔSOC_{int}). One hidden layer with ten nodes is used to train the model using a Bayesian regulation algorithm with the neural fitting tool in MATLAB. To confirm the accuracy of the surrogate model, the simulation results are compared with the surrogate measure using the 300 randomly selected sample points. Because the average error is 0.12 %, it should be noted that the use of a surrogate model can be an acceptable approach. To calculate a probabilistic function value, 50^3 times simulation results are required because 50 sample points of each driver's parameter (K, τ_{r}, τ_{n}) are used. In case of computational time to calculate the function value, the amount of time consumption using the dynamic simulation model is about 40,000 times using the surrogate model. Therefore, the surrogate model is essential to optimize the gear ratio in probabilistic approach.

4.3. Optimization Result

In the deterministic cases, the values of integrated SOC consumption are different among the driver models. Therefore, the cases of driver's parameter value covering the various driver's behaviors are selected to confirm the variation of optimal gear ratios. The parameter values for deterministic cases are shown in Table 3 and the results of the optimal gear ratios when using the deterministic and probabilistic approaches are summarized in Table 4.

As shown in Figure 11, when the values of K and τ_{r} become large, the integrated SOC consumption is sharply increased as the gear ratio increases. This means that the sensitivity of the integrated SOC consumption at a specific driving behavior is remarkably different among the gear ratios. Figure 12 shows the deterministic results with the various cases of the driver's parameter value selected from Table 3 and the probabilistic result. The integrated SOC consumptions and the optimal gear ratios are different among the cases of the deterministic approach. Hence, if the optimization of the gear ratio is only employed on a specific driver model case, this ratio may not be optimal for

Table 3. Deterministic driver's parameter values.

Parameter	Value			
	Case1	Case2	Case3	Case4
K	0.12	0.09	0.15	0.12
τ_{r}	0.35	0.2	0.45	0.45
τ_{n}	0.15	0.12	0.12	0.18

Table 4. Optimization results.

		Deterministic			
		Case1	Case2	Case3	Case4
Gear ratio	Initial	4.000			
	Optimal	5.173	5.320	3.755	4.663
ΔSOC_{int} (%)	Initial	3.889	3.657	4.511	4.208
	Optimal	3.766 (3.2 %↓)	3.544 (3.1 %↓)	4.503 (0.2 %↓)	4.152 (1.3 %↓)
		Probabilistic			
Gear ratio	Initial	4.000			
	Optimal	4.766			
$\int\Delta SOC_{\text{int}}$ (%)	Initial	3.846			
	Optimal	3.768 (2.0 % ↓)			

www.manaraa.com

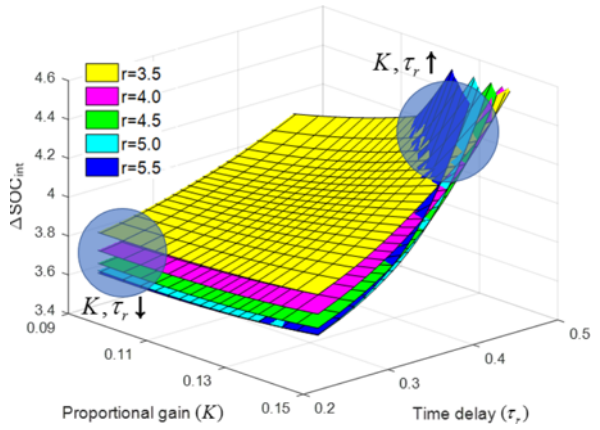

Figure 11. Results of integrated SOC consumption by K, τ_r, and r.

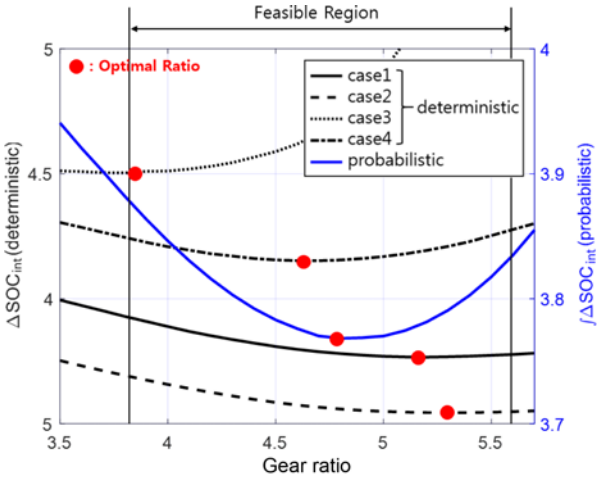

Figure 12. Comparison of integrated SOC consumption between deterministic and probabilistic approaches.

Table 5. Optimal gear ratios of each cycle.

Cycle	Deterministic				Proba-bilistic
	Case1	Case2	Case3	Case4	
UDDS	5.154	5.322	3.733	4.702	4.782
UDC	5.663	5.663	3.729	4.441	4.662
JC08	5.230	5.096	3.888	4.662	4.755
Range	0.509	0.567	0.159	0.261	0.120

the other cases. However, the optimization using the probabilistic approach can derive an optimal gear ratio that represents the overall driver's behavior. The optimal gear ratios of each cycle with respect to the deterministic and the probabilistic approaches are summarized in Table 5. With these optimal gear ratios, the results of miles per gallon gasoline equivalent (MPGe) evaluating the electric energy efficiency in the United States Environmental Protection Agency (EPA) are shown in Table 6. The ranges of the gear ratios and MPGe's in the deterministic approach are larger than those of the probabilistic approach except Case3. Since Case3 represents a driver with high aggression and slow perception, it leads to the excessive SOC consumption as shown in Figure 11. In this case, the driver's behavior is more dominant than the gear ratio for the SOC consumption so that the effect of optimal gear ratio for the SOC consumption is less than other cases. In terms of the robustness, these results show that the probabilistic approach is more reasonable than the deterministic approach. Therefore, the probabilistic approach should be employed to optimize the gear ratio regarding the variations in a real-world situation.

Table 6. MPGe's of each cycle.

Cycle	Deterministic				Proba-bilistic
	Case1	Case2	Case3	Case4	
UDDS	188	197	163	176	191
UDC	216	245	166	188	210
JC08	193	210	155	168	191
Range	28	48	11	20	19

5. CONCLUSION

This paper proposed a new method to optimize the gear ratio using a probabilistic driver model of an in-wheel motor vehicle. A dynamic model of an in-wheel motor vehicle and a probabilistic driver model were both developed to estimate the energy efficiency. A design problem was formulated to minimize the integrated SOC consumption with the dynamic constraints of the vehicle. A design example of an EV with two in-wheel motors to optimize the gear ratio was provided, the results of which showed the validity of the proposed method. In particular, by comparing the results of the optimal gear ratio between applying the deterministic and probabilistic driver models, the necessity of considering the probabilistic model can be seen.

ACKNOWLEDGEMENT–This research was supported by the Defense Acquisition Program Administration of Korea (DAPA) and by the Agency for Defense Development of Korea (ADD) (Grant No.: UC150014ID).

REFERENCES

Changyu, S., Lixia, W. and Qian, L. (2007). Optimization of injection molding process parameters using combination of artificial neural network and genetic algorithm method. *J. Materials Processing Technology*

www.manaraa.com

183, **2-3**, 412−418.

Day, T. D. and Metz, L. D. (2000). The simulation of driver inputs using a vehicle driver model. *SAE Paper No*. 2000-01-1313.

De Vlieger, I. (1997). On-board emission and fuel consumption measurement campaign on petrol-driven passenger cars. *Atmospheric Environment* **31**, **22**, 3753–3761.

Di Nicola, F., Sorniotti, A., Holdstock, T., Viotto, F. and Bertolotto, S. (2012). Optimization of a multiple-speed transmission for downsizing the motor of a fully electric vehicle. *SAE Int. J. Alternative Powertrains* **1**, **1**, 134–143.

Gao, B., Liang, Q., Xiang, Y., Guo, L. and Chen, H. (2015). Gear ratio optimization and shift control of 2-speed I-AMT in electric vehicle. *Mechanical Systems and Signal Processing*, **50-51**, 615−631.

Gorissen, D., Couckuty, I., Demeester, P., Dhaene, T. and Crombecq, K. (2010). A surrogate modeling and adaptive sampling toolbox for computer based design. *J. Machine Learning Research*, **11**, 2051−2055.

He, H., Xiong, R. and Fan, J. (2011). Evaluation of lithium-ion battery equivalent circuit models for state of charge estimation by an experimental approach. *Energies* **4**, **4**, 582–598.

Kannan, G. R., Balasubramanian, K. R. and Anand, R. (2013). Artificial neural network approach to study the effect of injection pressure and timing on diesel engine performance fueled with biodiesel. *Int. J. Automotive Technology* **14**, **4**, 507−519.

Kim, D., Shin, K., Kim, Y. and Cheon, J. (2010). Integrated design of in-wheel motor system on rear wheels for small electric vehicle. *World Electric Vehicle Journal* **4**, **3**, 597–602.

Kim, S. C., Kim, W. and Kim, M. S. (2013). Cooling performance of 25 kw in-wheel motor for electric vehicles. *Int. J. Automotive Technology* **14**, **4**, 559−567.

Ko, S., Song, C. and Kim, H. (2016). Cooperative control of the motor and the electric booster brake to improve the stability of an in-wheel electric vehicle. *Int. J. Automotive Technology* **17**, **3**, 447−456.

LeBlanc, D. J., Sivak, M. and Bogard, S. (2010). Using Naturalistic Driving Data to Assess Variations in Fuel Efficiency among Individual Drivers. The University of Michigan Transportation Research Institute. UMTRI-2010-34.

Lerspalungsanti, S., Albers, A., Ott, S. and Duser, T. (2015). Human ride comfort prediction of drive train using modeling method based on artificial neural networks. *Int. J. Automotive Technology* **16**, **1**, 153−166.

Lixin, S. (2009). Electric vehicle development: The past, present & future. *Proc. IEEE 3rd Int. Conf. Power Electronics Systems and Applications (PESA)*, Hong Kong, China.

Mahapatra, S., Egel, T., Hassan, R., Shenoy, R. and Carone, M. (2008). Model-based design for hybrid electric vehicle system. *SAE Paper No*. 2008-01-0085.

McGordon, A., Poxon, J. E., Cheng, C., Jones, R. P. and Jennings, P. A. (2011). Development of a driver model to study the effects of real-world driver behaviour on the fuel consumption. *Proc. Institution of Mechanical Engineers, Part D: J. Automobile Engineering* **225**, **11**, 1518–1530.

Noh, K. H., Rah, C. K., Yoon, Y. S. and Yi, K. S. (2014). Experimental approach to developing human driver models considering driver's human factors. *Int. J. Automotive Technology* **15**, **4**, 655−666.

Pi, J. M., Bak, Y. S., You, Y. K., Park, D. H. and Kim, S. H. (2016). Development of route information based driving control algorithm for a range-extended electric vehicle. *Int. J. Automotive Technology* **17**, **6**, 1101−1111.

Ren, Q., Crolla, D. A. and Morris, A. (2009). Effect of transmission design on electric vehicle performance. *Proc. IEEE Vehicle Power and Propulsion Conf*., Dearborn, Michigan, USA.

Reif, K. (2014). *Fundamentals of Automotive and Engine Technology*. Springer. Wiesbaden, Germany.

Son, J., Park, M., Won, K., Kim, Y., Son, S., McGordon, A., Jennings, P. and Birrell, S. (2016). Comparative study between Korea and UK: Relationship between driving style and real-world fuel consumption. *Int. J. Automotive Technology* **17**, **1**, 175−181.

Sorniotti, A., Subramanyan, S., Turner, A., Cavallono, C., Viotto, F. and Bertolotto, S. (2011). Selection of the optimal gearbox layout for an electric vehicle. *SAE Int. J. Engines* **4**, **1**, 1267–1280.

Wang, B., Choi, J. H., Song, H. W., Chol, H. K. and Hwang, S. H. (2014). Development of the performance simulator for electric scooters with an in-wheel motor. *Int. J. Automotive Technology* **15**, **5**, 835−841.

Wang, J., Wang, Q. N., Wang, P. Y., Wang, J. N. and Zou, N. W. (2015). Hybrid electric vehicle modeling accuracy verification and global optimal control algorithm research. *Int. J. Automotive Technology* **16**, **3**, 513−524.

Zhou, X., Walker, P. and Zhang, N. (2013). Performance improvement of a two speed EV through combined gear ratio and shift schedule optimization. *SAE Paper No*. 2013-01-1477.

www.manaraa.com

Reproduced with permission of copyright owner. Further reproduction prohibited without permission.

www.manaraa.com